International Journal Of
Industrial Electronics Control and Optimization
Print ISSN: 3517-2645
Online ISSN: 3568-2645
Homepage: https://ieco.usb.ac.ir/

Synchronization Control Strategy of Inverted Pendulums using Control Law Partitioning and Contraction Theory

Rogayyeh Soltani[1] | Bashir Naderi[1] | Saeed Nezhadhossein[1] | Aghileh Heydari[1]

Department of Mathematics, Payame Noor University, Tehran, Iran[1]
Corresponding author's email: b_naderi@pnu.ac.ir

Article Info

Article type:
Research Article
Article history:
Received: 15 March 2023
Revised: 14 Jun 2023
Accepted: 1 July 2023
Published online: 11 July 2023
Keywords:
Contraction Theory,
Synchronization Control,
Inverted Pendulum,
Cart and Pole.

ABSTRACT

A synchronization balancing control is proposed based on the contraction theory of stability. The control scheme is applied to balance an inverted pendulum mounted on a moving cart with two wheels. The equations of motion of the system are divided into two cascade systems using the control law partitioning method, which allows the designer to split the control design process into simpler parts for each isolated fragment of the system. Then two control laws are proposed for the corresponding partitions. The main aim of the closed-loop system is to balance the pendulum and synchronize the transient behavior of the system state with a reference model with time-varying parameters. The stability is guaranteed using the contraction theory. The proposed control mechanism is investigated through simulation and comparison studies, and the results confirm the performance and superiority of the proposed controller.

Nomenclature

x	State vector of system, $\mathbb{R}^{n\times 1}$	g	Gravity, $\mathbb{R}$
$f(.,.)$	Continuously differentiable function, $\mathbb{R}^{n\times 1}$	τ_R, τ_L	Right and left wheel torque, $\mathbb{R}$
$\partial/\partial x$	Partial differentiation with respect to x	τ_B	Applied torque to the pendulum joint, $\mathbb{R}$
δx	Perturbed variation to x	τ	Summation of the right and left wheel torque, $\mathbb{R}$
$J(x,t)$	Jacobian matrix of the system, $\mathbb{R}^{n\times n}$	θ	The rotational angle of the pendulum, $\mathbb{R}$
J_{sym}	The symmetric part of the Jacobian matrix, $\mathbb{R}^{n\times n}$	u	The output of the linear portion of the system, $\mathbb{R}$
λ_{max}	The largest eigenvalue of J_{sym}, $\mathbb{R}$	α_i, β_i, ξ	The defined parameter in Equs (14) and (15), $\mathbb{R}$
$I_{n\times n}$	The dimensional identity matrix, $\mathbb{R}^{n\times n}$	ψ	The defined variable based on the reference, $\mathbb{R}$
$\|.\|$	The Euclidian norm	m_B	Body weight, 1.2 kg
μ	A real positive fix constant, $\mathbb{R}$	m_W	Wheel weight, 0.02 kg
$\varphi(x,t)$	Transition matrix, $\mathbb{R}^{n\times n}$	I_B	Body inertia, 0.015 kgm^2
z	Generalized state vector, $\mathbb{R}^{n\times 1}$	I_W	Wheel inertia, 0.00002 kgm^2
M	A square symmetric metric, $\mathbb{R}^{n\times n}$	I_M	Rotor inertia, 0.000001 kgm^2
$F(x,t)$	Generalized Jacobian matrix, $\mathbb{R}^{n\times n}$	I_G	Gearbox inertia, 0.0001 kgm^2
X	The state vectors of the system, $\mathbb{R}^{n\times 1}$	b_M	Motor damping, 0.001 Nms/rad
Y	The state vector of the reference system, $\mathbb{R}^{n\times 1}$	b_W	Wheel damping, 0.001 Nms/rad
γ_i	Time-variant coefficients of the reference system, $\mathbb{R}$	b_G	Gearbox damping, 0.001 Nms/rad
e_i	synchronization error, $\mathbb{R}$	n	Gearbox ratio, 30
z_i	Generalized synchronization error variable, $\mathbb{R}$	r	Wheel diameter, 0.032 m
z_i^{ref}	a virtual desired value for z_i, $\mathbb{R}$	l	COG distance, 0.075 m
E	Error vector of synchronization system, $\mathbb{R}^{n\times 1}$	R	Armature resistance, 2.4 Ω
Z	Generalized Error vector of system, $\mathbb{R}^{n\times 1}$	K	Motor constant, 0.01 Nm/A
η_i	The desired dynamics design parameters	ζ_i	Design parameters of the error system dynamics

Copyright © 2023, Soltani et al..
Publisher: University of Sistan and Baluchestan

I. Introduction

Background: An Inverted Pendulum (IP) is a principal benchmark for control systems. IP Balancing control has been studied for decades due to its role in many other sciences, including the rocket's vertical take-off [1], biped robot walking analysis and control [2], self-balancing robot [3], dynamics of human sagittal balance [4], prosthetic finger robust controller design [5], lower limb rehabilitation robot [6], running trajectory generation [7], development of biomechanical gait analysis [8], dynamic walking of legged robots [9]. This wide range of applications makes the inverted pendulum an attractive research area, from theoretical analysis to practical control system design. Moreover, synchronization control is an active research area. Lyapunov stable fractional-order sliding mode controller with time-varying switching surface and without the reaching phase is proposed in [10]. Impulsive synchronization in fractional-order complex-valued reaction-diffusion networked systems based on the Lyapunov function, finite-time Mittag-Leffler criteria, and linear matrix inequalities (LMIs) as a cryptosystem is introduced in [11].

Literature review: In 2002, a moving IP as an archetype of a two-wheeled robot was presented [12]. As a result of its two coaxial wheels connected to two DC motors, the vehicle can turn without transitional motion. The controller was created with two state-space controllers connected to DC motors that drive the wheels by an isolation unit. In 2005, Ibanez et al. offered a nonlinear controller to balance an IP, which utilized partial feedback linearization [13]. The inverse pendulum excitation coordinates were linearized first, and then a Lyapunov-like function was designed to gain a stable feedback controller. In 2006, Muskinja and Tovornik developed an adaptive state controller to stabilize and optimally balance an IP, in which a switching mechanism between the swing and balance algorithm has been proposed [14]. In 2011, the optimal control of the nonlinear dynamic system of IP was proposed, using LQR and PID controllers [15]. In 2018, Khoshroo et al. designed a reinforcement learning controller based on the robust quadratic linear controller (LQR) for a four-degree-of-freedom inverted pendulum [16]. In 2018, Irfan proposed a robust control mechanism and compared it with time-dependent linear and nonlinear control methods, energy-based methods, and tracking controllers, to confirm the efficiency of IP control systems [17]. In 2018, Franco et al. introduced a balancing control mechanism for a kind of flexible IP, which was robust against external disturbances. In addition, a method was developed to identify the dominant parameters that impact the robustness of the closed-loop system [18]. In 2019, Hamza et al. used a rotational IP as a point of reference for a comparative study of different control methods, such as oscillation control, stabilization control, switching control, and path tracking control. Finally, they proposed a new general system for testing higher-order intelligent controllers [1]. In 2020, Johnson et al. implemented a perceptual controller for an IP on a cart. Perceptual control theory roots in a theory that says "behavior is the control of perception." A unique feature of this controller is facing external disturbance [19]. In 2023, stabilization of an IP on a cart with cart position feedback was considered in [20]. Stable and proper compensators are not able to stabilize such a system. Therefore, the paper suggested utilizing an additional compensator in a parallel feedforward loop. The suggestion brought up a high sensitivity to noise. In 2023, two reinforcement learning algorithms, i.e. basic Q-Learning and Deep Q-Networks, were utilized to balance an IP without mathematical model requirement [21]. The attained advantage was the practical applicability of the method. However, the disadvantages of it were the time required for training the controller and the complexity of the approach. An adaptive fuzzy fast terminal sliding mode controller was detailed in [22] to balance an IP on a cart in the presence of uncertainties and actuator faults. The method succeeded in balancing the IP while compensating for the imperfections with a fast transient response. However, the design procedure and stability proof analysis were complicated. A mathematical controller was designed for an IP based on Taylor expansion, fourth-order Runge–Kutta, and multiple time-scale perturbation techniques [23]. The linearized stability has been proven based on Routh–Hurwitz criterion. However, the difficulty of the design process, linearized stability, and sensitivity to uncertainties were the drawbacks of the method.

Research gap and motivation: However, the main issue in the control design is stability. The second method of Lyapunov for stability explicitly necessitates defining or finding a function as a distance metric. This metric function must be decreasing over time for guaranteed stability. In order to find this function, the system must have specific characteristics in its structure or involve implicit optimization. To solve this problem, contraction theory utilizes a differentially constructed distance function that is not explicitly defined [24]. The only required property for constructing the contraction metric is the stabilizability of the under-control system, or in other words, the existence of the control signal [24], [25]. This generalization enables the contraction metric to be applied to underactuated systems. The other wide usage of the contraction theory is in transfer learning, in which a controller is designed for a typical system and must be tuned to work in the presence of uncertainty or parameter variations [24]. The contraction metric measures the convergence of two systems' trajectories [26]. Contraction theory, as stated in [27]-[29], is a study of the convergence of all nearby trajectories to a nominal motion. Therefore, this differential analysis is much simpler than what happened in Lyapunov's theory. A "contracting nonlinear dynamical system" is a term assigned to a system that exponentially forgets its initial conditions or external disturbances and

returns to its nominal trajectory fast [26]. The stability is different from the specific trajectory, which this fact is applied to the control designing process. In order to convergence checking, contraction theory utilized the neighboring system trajectories' local analysis [25]. For example, synchronization condition based on the contraction analysis is developed in [26], [30].

Challenges: The existing synchronization methods are trapped in high run-time computational cost or hard controller design procedure when seeking high accuracy, e.g. fractional order controllers or iterative methods ([11], [20]-[23]), or have lost the analysis of convergence whenever they proposed a simple controller, e.g. linear stable controller proposed in [31]. Finding the second derivative of the Lyapunov-like functions to prove stability is a complex task. Therefore, some methods suffer from the lack of guaranteed stability. In addition, the contraction-based synchronization controllers are applied to fully actuated systems, where the symmetric part of the Jacobian matrix is uniformly negative definite. However, in the underactuated systems, the symmetric part of the Jacobian matrix may not be uniformly negative definite. Here, the asymptotic convergence of such systems is studied. Moreover, time-varying parameters in the reference model are less studied in the literature.

Contributions: The contributions of this research can be listed as follows. (I) A balancing controller is designed for a benchmark, a two-wheeled self-balancing inverted pendulum robot, using a contraction-based synchronization procedure inspired by the works of [26] and [30]. (II) Time-varying parameters are considered for the synchronization reference model, which is different from the parameters of the under-control system, whereas in [26] and [30], the parameters of the reference model are time-invariant, and their values are as same as those of the under-control system. (III) In addition, the under-control system is underactuated, so the symmetric part of its Jacobian matrix is not uniformly negative definite. (IV) The exponential convergence of the generalized state variables to zero and the asymptotic stability of the closed-loop synchronization system are guaranteed. (V) Control law partitioning is utilized to separate the control design process into two simpler mechanisms, the linear control portion (with a perfect control design based on transfer function) and the synchronization control law (which provides an underactuated affine system). (VI) the main achievements of the proposed control method are ease of design, low runtime computational cost, guaranteed stability with exponential convergence, adjustable desired transient response, small synchronization error, and the ability of experimental implementation due to its simplicity. These specifications make the proposed method applicable to control fast dynamics including biped walking robots, human gait and running balance, or rehabilitation robotics.

Paper organization: In this paper, Section 2 briefly introduces the contraction theory. Then in Section 3, we present the equations of motion of the two-wheeled IP system. In Section 4, we propose a control law partitioning method in combination with contraction theory based on synchronization applied to the balancing control. Section 5 investigates the performance of the proposed controller through simulation and comparison studies (compared with the method proposed in [32]). The conclusion is stated in Section 6.

II. Preliminaries

In this section, the fundamental definitions of the contraction theory are formulated [26], [27]. Then we will briefly discuss the generalized distance measure, generalized eigenvalue analysis, and the control law partitioning approach.

A. Contraction Theory

Let's consider an autonomous nonlinear dynamical system,

$$\dot{x} = f(x,t), \tag{1}$$

in which, $f(.,.)$ is an $n \times 1$ continuously differentiable vector function and $x \in \mathbb{R}^{n\times 1}$is the state vector of system. If the system's state vector is perturbed by an infinitesimal shift of δx, also termed virtual displacement, then based on the concept of virtual dynamics, the first variation of the system will be as follows [26]:

$$\delta\dot{x} = \frac{\partial f(x,t)}{\partial x}\delta x\,. \tag{2}$$

Equation (2) determines the way the system reacts to the virtual displacement in the future. In other words, the variation in the trajectory, which is due to the infinitesimal shift in the initial value, is investigated by the virtual dynamic theory. Therefore, there are two different trajectories, including nominal (x) and perturbed $(x+\delta x)$. The quadratic distance between these two neighboring trajectories can be measured with $\delta x^T\delta x$. The behavior of convergence/divergence between the trajectories can be studied through their quadratic distance as follows:

$$\frac{d}{dt}(\delta x^T\delta x) = 2\delta x^T\delta\dot{x} = 2\delta x^T\frac{\partial f(x,t)}{\partial x}\delta x\,. \tag{3}$$

If $J(x,t) = \partial f/\partial x$ is the Jacobian matrix of the system and $J_{sym} = \frac{1}{2}\left(\frac{\partial f(x,t)}{\partial x} + \frac{\partial f(x,t)}{\partial x}^T\right)$ is its symmetric part, then $\lambda_{max}(x,t)$ is the largest eigenvalue of J_{sym} such that $\frac{\partial f(x,t)}{\partial x} \le \lambda_{max}(x,t)I_{n\times n}$. Therefore,

$$\frac{d}{dt}(\delta x^T\delta x) \le 2\lambda_{max}(x,t)(\delta x^T\delta x)\,. \tag{4}$$

Then, it can be proved that

$$\|\delta x(t)\| \le \|\delta x(0)\|e^{\int_0^t \lambda_{max}(x,t)dt}\,. \tag{5}$$

According to the $\lambda_{max}(x,t)$, the converging system is defined in [27] as follows.

Remark 1: Every infinitesimal perturbation, $\|\delta x\|$, will exponentially converge to zero if $\lambda_{max}(x,t)$ is strictly uniformly negative, which means that

$$\exists\mu > 0, \forall x, \forall t > 0 \rightarrow \lambda_{max}(x,t) \le -\mu. \tag{6}$$

Based on remark 1, when the Jacobian matrix, $J(x,t)$, is uniformly negative definite in a region, the system is termed "contracting" in that region [26], [27].

Remark 2: If a system is contracting in whole state space, then global exponential convergence of the perturbed

trajectories to the nominal trajectory is guaranteed [26]. Hence, the system is contracting if

$$\exists \mu > 0, \forall x, \forall t > 0 \rightarrow J_{sym} \leq -\mu I_{n\times n} < 0\,. \tag{7}$$

Fig. 1 shows the concept of trajectory perturbation, distance, and convergence. The above-mentioned concept is the basis of contraction theory.

B. Distance measure generalization

If we generalize the distance definition, we can widely generalize the contraction theory. The generalized distance can be explained by the differential coordination transition as

$$\delta z = \varphi(x,t)\delta x, \tag{8}$$

in which, $\varphi(x,t)$ is a transition matrix, such that $M = \theta^T\theta$ is a square symmetric differential continuous metric. This transition leads to a generalization of distance and the quadratic distance $\delta z^T\delta z = \delta x^T M \delta x$. The convergence of δz to zero brings the convergence of δx to zero [26].

C. Generalized eigenvalue analysis

Time derivative of (8) is

$$\begin{aligned}\frac{d}{dt}\delta z &= \dot{\varphi}(x,t)\delta x + \varphi(x,t)\frac{d}{dt}\delta x \\ &= \left(\dot{\varphi} + \varphi\frac{\partial f}{\partial x}\right)\varphi^{-1}\delta z = F(x,t)\delta z,\end{aligned} \tag{9}$$

in which, $F(x,t) = \left(\dot{\varphi} + \varphi\frac{\partial f}{\partial x}\right)\varphi^{-1}$ is the generalized Jacobian matrix. Therefore,

$$\frac{d}{dt}(\delta z^T\delta z) = 2\delta z^T\frac{d}{dt}\delta z = 2\delta z^T F(x,t)\delta z\,. \tag{10}$$

As before, if $F(x,t)$ is strictly negative definite, then the convergence of δz, and consequently δx, to zero is guaranteed. Here, we used contraction theory to synchronize two nonlinear systems [26].

D. Control Law Partitioning

Designing a controller for a complex nonlinear system is a complicated task. Control Law Partitioning (CLP) approach departs the control law into two portions to simplify the control design procedure. The most famous CLP method dissects the control law into a model-based controller and the servo feedback [33], [34]. The model-based control law transforms the system into a unit mass for the servo controller [33], [34]. There are other kinds of CLP, for example, layered architecture [29], [35], where the controller is partitioned based on the task. Here, we utilize CLP to separate the system's model into a transfer function and a simple affine system.

III. System Modeling and Control Law Partitioning

This section describes the mathematical model of the two-wheeled self-balancing robot or simply an inverted pendulum attached to a two-wheeled moving cart [3]. The schematic of the system is drawn in Fig. 2.

A. Dynamical Model of the System

The mathematical model of the system is described as:

$$\left(m_B + 2m_w + 2\frac{I_w}{r^2}\right)\ddot{p} + 2\frac{b_w}{r^2}\dot{p} + m_B l\ddot{\theta} = \frac{1}{r}(\tau_R + \tau_L) \tag{11.a.}$$

$$m_B l\ddot{p} + (m_B l^2 + I_B)\ddot{\theta} - m_B lg\theta = -(\tau_R + \tau_L) \tag{11.b.}$$

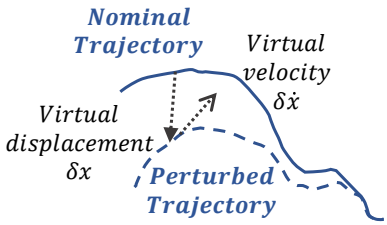


Fig. 1. The concept of neighboring trajectories, virtual displacement, distance, and convergence

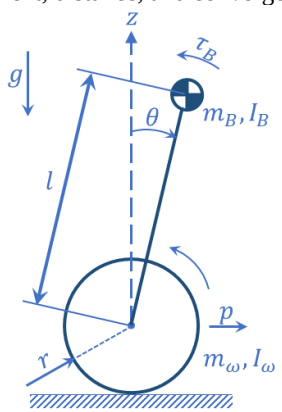


Fig. 2. Schematic of the dynamical system (two-wheeled self-balancing robot driven by dc gear motors) [3]

It is assumed that small movements of the cart (p) along axis x cause a neglectable deviation in the rotational angle of the pendulum, θ, [3]. In other words, when the cart is moving along x direction $\dot{\theta} \approx 0$ and $\cos(\theta) \approx 1$. Here, τ_B, τ_R, and τ_L are the applied torque to the pendulum joint and right and left wheels torques, respectively. Parameters of the system are selected as described in the nomenclature section.

Defining $\tau = \tau_R + \tau_L$, based on (11.b.) the cart acceleration $\ddot{p}$ can be computed.

$$\ddot{p} = -\left(l + \frac{I_B}{m_B l}\right)\ddot{\theta} + g\theta - \frac{1}{m_B l}\tau\,. \tag{12}$$

Substituting (12) in (11.a.), the following equation will be obtained.

$$\begin{aligned}&\left(m_B^2 l^2 - \left(m_B + 2m_w + 2\frac{I_w}{r^2}\right)(m_B l^2 + I_B)\right)\ddot{\theta} \\ &\quad - \left(2\frac{b_w}{r^2}(m_B l^2 + I_B)\right)\dot{\theta} \\ &\quad + \left(\left(m_B + 2m_w + 2\frac{I_w}{r^2}\right)m_B lg\right)\theta \\ &\quad + \left(2m_B lg\frac{b_w}{r^2}\right)\int_0^t \theta dt \\ &= \left(\frac{m_B l}{r} + \left(m_B + 2m_w + 2\frac{I_w}{r^2}\right)\right)\tau \\ &\quad + \left(2\frac{b_w}{r^2}\right)\int_0^t \tau dt\,.\end{aligned} \tag{13}$$

For the sake of simplicity, we rename the constant coefficients as below,

$$\begin{cases} \beta_1 = -\xi^{-1}\left(2m_B lg\frac{b_w}{r^2}\right), \\ \beta_2 = -\xi^{-1}\left(\left(m_B + 2m_w + 2\frac{I_w}{r^2}\right)m_B lg\right), \\ \beta_3 = \xi^{-1}\left(2\frac{b_w}{r^2}(m_B l^2 + I_B)\right), \\ \alpha_1 = \xi^{-1}\left(\frac{m_B l}{r} + \left(m_B + 2m_w + 2\frac{I_w}{r^2}\right)\right), \\ \alpha_2 = \xi^{-1}\left(2\frac{b_w}{r^2}\right), \end{cases} \quad (14)$$

in which,

$$\xi = \left(m_B^2 l^2 - \left(m_B + 2m_w + 2\frac{I_w}{r^2}\right)(m_B l^2 + I_B)\right). \quad (15)$$

Therefore, the equation of motion is rewritten.

$$\ddot{\theta} - \beta_3\dot{\theta} - \beta_2\theta - \beta_1\int_0^t \theta dt = \alpha_1\tau + \alpha_2\int_0^t \tau dt\,. \quad (16)$$

The main aim of the controller design procedure is to find the control signal, τ, such that the dynamical system behaves desirably.

B. Control Design Partitioning

In order to simplify the control design process, we proposed using "Control Law Partitioning," in which the obtained equation of motion can be divided into two cascade systems. Therefore, two control laws will be designed separately. In fact, the designed controller consists of two parts, a Synchronization Control Law (SCL) and a first-order Linear Control Portion (LCP). To simplify the control design process, we propose the linear portion of the system as below:

$$u = \alpha_1\tau + \alpha_2\int_0^t \tau dt\,. \quad (17)$$

Equation (17) is a first-order differential equation with constant coefficients. Therefore, τ can be easily found according to the new control signal, u. The proposed Linear Control Portion (LCP) is designed based on (17), as below:

$$\frac{\tau(s)}{u(s)} = \frac{s}{\alpha_1 s + \alpha_2}. \quad (18)$$

Since the angular position of the inverted pendulum is important to be synchronized with a desired reference system, one can define the state variables of the system as $X_1 = \int_0^t \theta dt$, $X_2 = \theta$, and $X_3 = \dot{\theta}$, the state vector as $X = [X_1, X_2, X_3]^T$, and the state space as below:

$$\begin{cases} \dot{X}_1 = X_2\,, \\ \dot{X}_2 = X_3\,, \\ \dot{X}_3 = \beta_1 X_1 + \beta_2 X_2 + \beta_3 X_3 + u\,. \end{cases} \quad (19)$$

Therefore, (19) is the synchronizing portion of the system. In the next section, we will formulate the control design process for (19).

IV. Contraction-based Synchronization

In this section, we proposed a Synchronization Control Law (SCL) based on the contraction theory [26]. First of all, a desired reference system is introduced as:

$$\begin{cases} \dot{Y}_1 = Y_2\,, \\ \dot{Y}_2 = Y_3\,, \\ \dot{Y}_3 = \gamma_1 Y_1 + \gamma_2 Y_2 + \gamma_3 Y_3\,, \end{cases} \quad (20)$$

in which, $Y = [Y_1, Y_2, Y_3]^T$ is the state vector of the reference system, and γ_1, γ_2 and γ_3 are (time-variant/invariant) coefficients of the reference system, which are adjusted for achieving the desired transient response. In this paper, we utilized time-variant coefficients for the reference model. Synchronization error is defined as $e_1 = X_1 - Y_1$, $e_2 = X_2 - Y_2$, and $e_3 = X_3 - Y_3$. By subtracting (20) from (19), we have:

$$\begin{cases} \dot{e}_1 = e_2\,, \\ \dot{e}_2 = e_3\,, \\ \dot{e}_3 = \beta_1 e_1 + \beta_2 e_2 + \beta_3 e_3 + \psi + u\,, \end{cases} \quad (21)$$

in which, $\psi = (\beta_1 - \gamma_1)Y_1 + (\beta_2 - \gamma_2)Y_2 + (\beta_3 - \gamma_3)Y_3$. Now, the control law will be designed through three steps based on the contraction theory. We define a new variable $z_1 \triangleq e_1$. Considering a desired dynamic of z_1 as $\dot{z}_1^{ref} = -\eta_1 z_1$, in which z_1^{ref} is a virtual desired value for z_1, and comparing with its actual dynamics $\dot{z}_1 = \dot{e}_1 = e_2$, a desired value for e_2 is obtained as $e_{2d} = -\eta_1 z_1$. Here, a new conceptual error is defined as:

$$z_2 \triangleq e_2 - e_{2d} = \eta_1 e_1 + e_2\,. \quad (22)$$

When z_2 converges to 0, considering (22), e_2 will converge to e_{2d}, which means that $(\dot{e}_1 + e_1) \to 0$ that is a desired behavior. Based on (22), we have:

$$e_2 = z_2 - \eta_1 z_1\,. \quad (23)$$

and the dynamic of z_2 is computable as:

$$\dot{z}_2 = -\eta_1^2 z_1 + \eta_1 z_2 + e_3\,. \quad (24)$$

However, the desired dynamic is $\dot{z}_2^{ref} = -\eta_2 z_2$. Therefore, a new desired value for e_3 can be obtained as $e_{3d} = -\eta_1\eta_2 e_1 - (\eta_1 + \eta_2)e_2$ based on (24) and $\dot{z}_2^{ref}$. The other conceptual error is defined as:

$$z_3 \triangleq e_3 - e_{3d} = \eta_1\eta_2 e_1 + (\eta_1 + \eta_2)e_2 + e_3\,. \quad (25)$$

To push z_3 to zero, its dynamic is computed:

$$\dot{z}_3 = \eta_1\eta_2 e_2 + (\eta_1 + \eta_2)e_3 + \beta_1 e_1 + \beta_2 e_2 + \beta_3 e_3 + \psi + u\,. \quad (26)$$

However, the desired dynamic is $\dot{z}_3^{ref} = -\eta_3 z_3$. Thus, by $\dot{z}_3 \to \dot{z}_3^{ref}$, we have:

$$\eta_3 z_3 + \eta_1\eta_2 e_2 + (\eta_1 + \eta_2)e_3 + \beta_1 e_1 + \beta_2 e_2 + \beta_3 e_3 + \psi + u = 0. \quad (27)$$

Now, we can propose the synchronization control law as:

$$\begin{aligned} u = &-\psi - (\eta_1\eta_2\eta_3 + \beta_1)e_1 \\ &-\left((\eta_1\eta_2 + \eta_1\eta_3 + \eta_2\eta_3) + \beta_2\right)e_2 \\ &-\left((\eta_1 + \eta_2 + \eta_3) + \beta_3\right)e_3\,. \end{aligned} \quad (28)$$

The block diagram of the proposed controller for the closed-loop synchronization system is depicted in Fig. 3.

This controller design procedure roots in the contraction theory and guarantees the stability of the closed-loop system. In this paper, we defined the state vector of the closed-loop system as $E = [e_1, e_2, e_3]^T$ and the generalized state vector as $Z = [z_1, z_2, z_3]^T$, therefore, the state generalization (coordination transition) is:

$$Z = \varphi E\,, \quad (29)$$

in which,

$$\varphi = \begin{bmatrix} 1 & 0 & 0 \\ \eta_1 & 1 & 0 \\ \eta_1\eta_2 & \eta_1 + \eta_2 & 1 \end{bmatrix}. \quad (30)$$

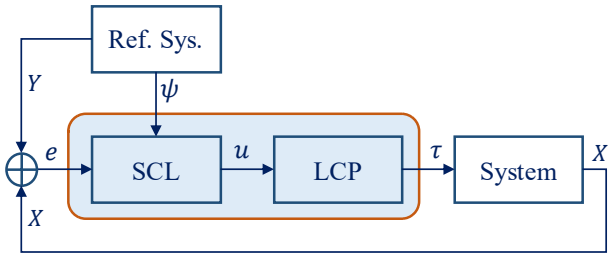


Fig. 3. Block diagram of the proposed controller for the closed-loop synchronization system

Considering (21) and (28), the closed-loop system can be rewritten as:

$$\dot{E} = \begin{bmatrix} 0 & 1 & 0 \\ 0 & 0 & 1 \\ -\zeta_1 & -\zeta_2 & -\zeta_3 \end{bmatrix} E \tag{31}$$

in which, $\zeta_1 = (\eta_1\eta_2\eta_3)$, $\zeta_2 = (\eta_1\eta_2 + \eta_1\eta_2 + \eta_1\eta_2)$, $\zeta_1 = (\eta_1 + \eta_2 + \eta_3)$. In addition, the generalized system is

$$\dot{Z} = \begin{bmatrix} \dot{z}_1 \\ \dot{z}_2 \\ \dot{z}_3 \end{bmatrix} = \begin{bmatrix} -\eta_1 & 1 & 0 \\ 0 & -\eta_2 & 1 \\ 0 & 0 & -\eta_3 \end{bmatrix} Z\,. \tag{32}$$

Therefore, Jacobian of the system is

$$J = \frac{\partial f(E)}{\partial E} = \begin{bmatrix} 0 & 1 & 0 \\ 0 & 0 & 1 \\ -\zeta_1 & -\zeta_2 & -\zeta_3 \end{bmatrix}. \tag{33}$$

The generalized Jacobian is

$$F = \left(\dot{\varphi} + \varphi \frac{\partial f(E)}{\partial E}\right)\varphi^{-1} = \begin{bmatrix} -\eta_1 & 1 & 0 \\ 0 & -\eta_2 & 1 \\ 0 & 0 & -\eta_3 \end{bmatrix}, \tag{34}$$

which is a uniformly negative definite matrix. Therefore, based on the contraction theory, applying the proposed controller, the generalized state (Z) exponentially converges to zero. In addition, since the largest eigenvalue of the symmetric part of the Jacobian matrix ($J = \partial f(E)/\partial E$) is not uniformly strictly negative, the synchronization error dynamics (E) is not exponentially convergent but it is asymptotically stable. Therefore, the synchronization error will converge to zero, despite the initial condition and the reference model. Fig. 4 shows the exponential stability of the generalized state, in which, 1000 runs of the generalized system's trajectory are drawn in gray lines in comparison to the exponential contraction (the largest eigenvalue of the symmetric part of the generalized Jacobian matrix, F).

V. Simulation

In this section, the proposed controller is applied to control the inverted pendulum that is described in section three. The initial conditions of the main system and the reference model are selected with normal random numbers in $[-1, +1]$. The reference model is the same as Eq. (20) with the following time-varying parameters:

$$\begin{cases} \gamma_1 = -1 - \big(2 - sin(5t)\big)e^{-\frac{1}{7}t}, \\ \gamma_2 = -3 - \big(2 - sin(3t)\big)e^{-\frac{1}{9}t}, \\ \gamma_3 = -3 - \big(2 - sin(2t)\big)e^{-\frac{1}{3}t}, \end{cases} \tag{35}$$

To evaluate the performance of the proposed control method, we provide several simulations and comparisons in Matlab/Simulink 2017a in Windows 10. The Simulink blocks are illustrated in Fig. 5.

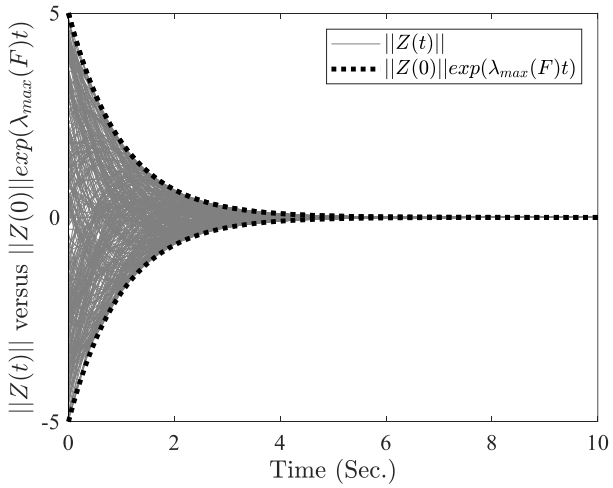


Fig. 4. Exponential convergence of the generalized state

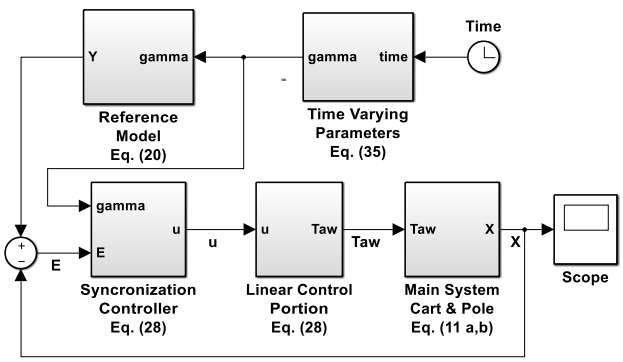


Fig. 5. Simulink blocks of the proposed control method

For a desired closed-loop system dynamics, we set the $\eta_1 = \eta_2 = \eta_3 = 3$. The tracking performance of the closed-loop control system is illustrated in Fig. 6, which shows that the system follows the reference model, which means that all three state variables track the corresponding state from the reference model. Note that there is only one control signal. As proposed in this paper, the controller is first partitioned into two portions, a state-space synchronization control law (SCL) and a linear control portion (LCP). The error is first handed into the SCL, where the signal u is produced, then the LCP converts u to τ as the actual control signal. These two signals are depicted in Fig. 7. The main features of the control signal are its boundedness and smoothness. The trajectory of the reference model and the actual system is drawn in Fig. 8. Since the steady-state response stays at the origin and the curve shows the states' movements, this trajectory illustrates the system's transient response. Since the system is a third-order dynamical system, its trajectory is also drawn in 3D space in Fig. 9 for better illustration. As seen in Fig. 8 and 9, although the initial condition of the two systems is completely random and different, the system follows the reference model. As a comparison study, the proposed method is compared with a recent similar method entitled "Nonlinear Model Predictive Controller Based on Particle Filter: Processor in the Loop Implementation" [32], which is based on particle filters containing normal random sequences of control signals. Weights are assigned to the particles based on their performance in predictive control.

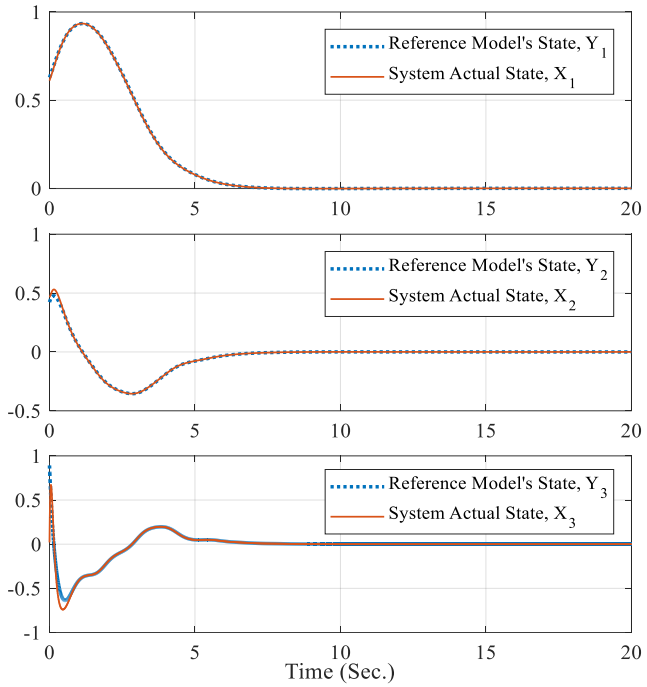


Fig. 6. Reference model synchronization control

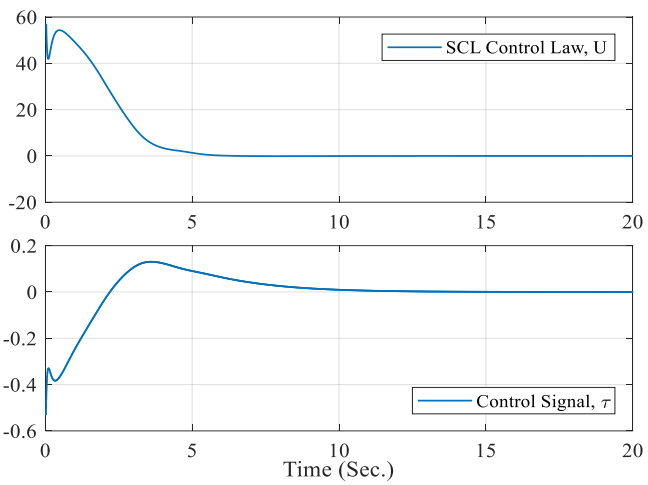


Fig. 7. Control Signals (u and τ)

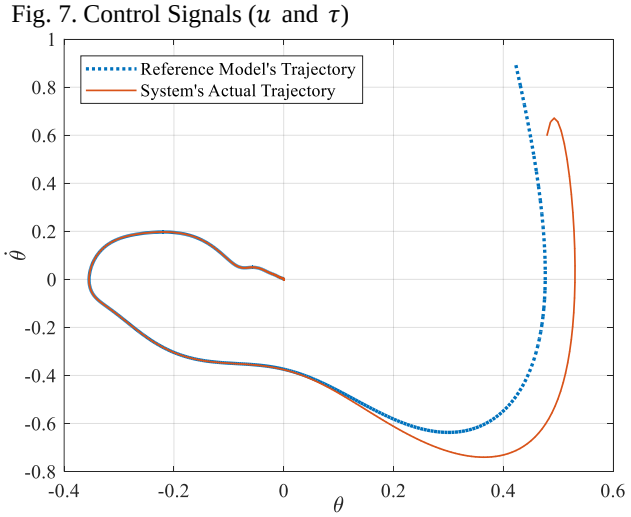


Fig. 8. Trajectory Tracking

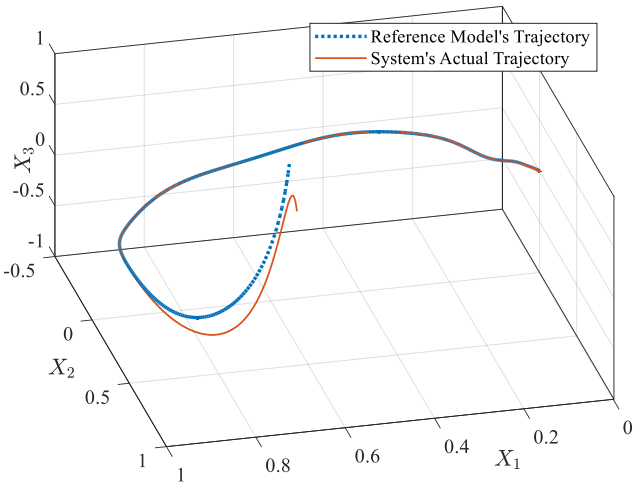


Fig. 9. 3D Trajectory Tracking

The resampling technique is utilized to provide the final control signal from the weighted particles. We simulated the method with 300 particles, a prediction horizon of 10 samples, and random initial weighting factors. The synchronization performances of the two methods are illustrated in Fig. 10, which shows that the proposed method has better performance rather than the compared method. Note that the runtime computational cost of our proposed method is far less than similar methods. The synchronization error is also drawn in Fig. 11, which shows the superiority of the proposed method. Moreover, the maximum value of the proposed control signal is 85.7951, while this value is 96.4092 for the comparative control signal. In general, the superiority of our proposed method can be observed in three perspectives, including (1) better synchronization performance and less error, (2) lower runtime computational cost, and (3) an easier design process.

VI. Conclusions

We proposed a synchronization controller based on contraction theory and control law partitioning for an underactuated two-wheeled self-balancing IP mobile robot. The proposed mechanism consists of a control law partitioning, which divides the control law into two parts, a linear transfer function and a synchronization control system designed based on contraction theory. The reference model is time-varying. The exponential convergence of the generalized state variables to zero and the asymptotic stability of the closed-loop synchronization system are proved. The main achievements of the proposed control method are ease of design, low runtime computational cost, guaranteed stability with exponential convergence, adjustable desired transient response, small synchronization error, and finally the ability of experimental implementation due to its simplicity. The proposed method is applicable for every dynamical system from chaotic to industrial robotics. The comparison study confirms the superiority of the method. In future studies, we will investigate the proposed mechanism for some chaotic mappings.

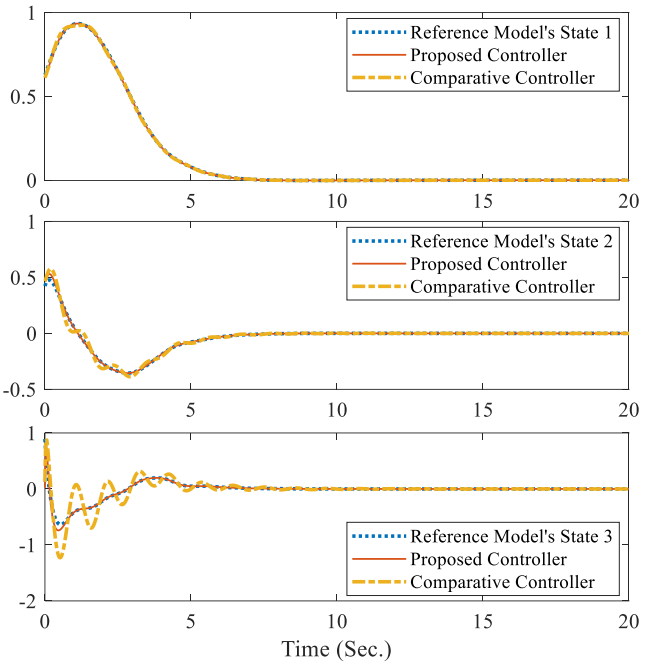


Fig. 10. Comparison study on synchronization performance

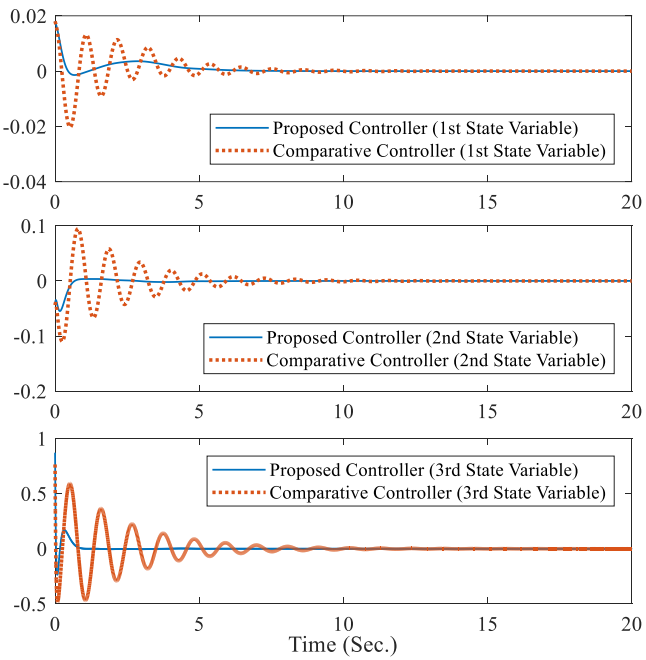


Fig. 11. Comparison study on synchronization error

REFERENCES

[1] M. F. Hamza, H. J. Yap, I. A. Choudhury, A. I. Isa, A. Y. Zimit, and T. Kumbasar, "Current development on using Rotary Inverted Pendulum as a benchmark for testing linear and nonlinear control algorithms," *Mech Syst Signal Process*, vol. 116, pp. 347–369, 2019, doi: https://doi.org/10.1016/j.ymssp.2018.06.054.

[2] S. Gora, S. S. Gupta, and A. Dutta, "Energy-Based Footstep Planning of Biped on Uneven Deformable Terrain Using Nonlinear Inverted Pendulum," J. Mech. Robot., vol. 15, no. 5, Nov. 2022.

[3] P. Frankovský, L. Dominik, A. Gmiterko, I. Virgala, P. Kurylo, and O. Perminova, "Modeling of Two-Wheeled Self-Balancing Robot Driven by DC Gearmotors," *International Journal of Applied Mechanics and Engineering*, vol. 22, no. 3, pp. 739–747, 2017, doi: doi:10.1515/ijame-2017-0046.

[4] M. van Mierlo, M. Vlutters, E. H. F. van Asseldonk, and H. van der Kooij, "Sagittal-plane balance perturbations during very slow walking: Strategies for recovering linear and angular momentum," J. Biomech., vol. 152, p. 111580, 2023.

[5] M. H. Jali, T. A. Izzuddin, R. Ghazali, C. C. Soon, and F. N. Zohedi, "Robust Controller Design with Particle Swarm Optimization for Nonlinear Prosthetic Hand System," *International Journal of Mechanical Engineering and Robotics Research*, vol. 6, no. 5, pp. 406–412, 2017, doi: https://doi.org/10.18178/ijmerr.6.5.406-412.

[6] M. Jalaeian-F., M. M. Fateh, and M. Rahimiyan, "Bi-Level Adaptive Computed-Current Impedance Controller for Electrically Driven Robots," *Robotica*, vol. 39, no. 2, pp. 200–216, May 2020, doi: 10.1017/S0263574720000314.

[7] S. Hanasaki, Y. Tazaki, H. Nagano, and Y. Yokokohji, "Running Trajectory Generation Including Gait Transition between Walking Based on the Time-Varying Linear Inverted Pendulum Mode," in *2022 IEEE-RAS 21st International Conference on Humanoid Robots (Humanoids)*, 2022, pp. 851–857. doi: 10.1109/Humanoids53995.2022.10000112.

[8] A. I. Tătaru and M. I. Baritz, "Development of biomechanical gait analysis based on inverted pendulum theory," *IOP Conf Ser Mater Sci Eng*, vol. 1256, no. 1, p. 12006, 2022, doi: 10.1088/1757-899X/1256/1/012006.

[9] J. Torres-Figueroa, E. A. Portilla-Flores, J. A. Vásquez-Santacruz, E. Vega-Alvarado, and L. F. Marín-Urías, "A Novel General Inverse Kinematics Optimization-Based Solution for Legged Robots in Dynamic Walking by a Heuristic Approach," *IEEE Access*, vol. 11, pp. 2886–2906, 2023, doi: 10.1109/ACCESS.2023.3234315.

[10] P. Narayanan, G.; Syed Ali, M.; Iqbal, Mohammed Mujtaba; Kumar, "Synchronization of fractional-order permanent magnet synchronous generator model based on terminal sliding mode control with switching surface," Math. Eng. Sci. Aerosp., vol. 12, no. 3, pp. 655–667, 2021.

[11] G. Narayanan, G. Muhiuddin, M. S. Ali, A. A. Z. Diab, J. F. Al-Amri, and H. I. Abdul-Ghaffar, "Impulsive Synchronization Control Mechanism for Fractional-Order Complex-Valued Reaction-Diffusion Systems With Sampled-Data Control: Its Application to Image Encryption," *IEEE Access*, vol. 10, pp. 83620–83635, 2022.

[12] F. Grasser, A. D'Arrigo, S. Colombi, and A. C. Rufer, "JOE: A mobile, inverted pendulum," *IEEE Transactions on Industrial Electronics*, vol. 49, no. 1, 2002, doi: 10.1109/41.982254.

[13] C. A. Ibañez, O. G. Frias, and M. S. Castañón, "Lyapunov-Based Controller for the Inverted Pendulum Cart System," *Nonlinear Dyn*, vol. 40, no. 4, pp. 367–374, 2005, doi: 10.1007/s11071-005-7290-y.

[14] N. Muskinja and B. Tovornik, "Swinging up and stabilization of a real inverted pendulum," *IEEE Transactions on Industrial Electronics*, vol. 53, no. 2, pp. 631–639, 2006, doi: 10.1109/TIE.2006.870667.

[15] L. B. Prasad, B. Tyagi, and H. O. Gupta, "Optimal control of nonlinear inverted pendulum dynamical system with disturbance input using PID controller & LQR," in *2011*

IEEE International Conference on Control System, Computing and Engineering, 2011, pp. 540–545. doi: 10.1109/ICCSCE.2011.6190585.
[16] M. Khoshroo, M. Eftekhari, and M. Eftekhari, "Reinforcement learning control of four degree of freedom inverted pendulum," *mdrsjrns*, vol. 18, no. 1, pp. 388–396, Mar. 2018.
[17] S. Irfan, A. Mehmood, M. T. Razzaq, and J. Iqbal, "Advanced sliding mode control techniques for Inverted Pendulum: Modelling and simulation," *Engineering Science and Technology, an International Journal*, vol. 21, no. 4, pp. 753–759, 2018, doi: https://doi.org/10.1016/j.jestch.2018.06.010.
[18] E. Franco, A. Astolfi, and F. Rodriguez y Baena, "Robust balancing control of flexible inverted-pendulum systems," *Mech Mach Theory*, vol. 130, pp. 539–551, 2018, doi: https://doi.org/10.1016/j.mechmachtheory.2018.09.001.
[19] T. Johnson, S. Zhou, W. Cheah, W. Mansell, R. Young, and S. Watson, "Implementation of a Perceptual Controller for an Inverted Pendulum Robot," *J Intell Robot Syst*, vol. 99, no. 3, pp. 683–692, 2020, doi: 10.1007/s10846-020-01158-4.
[20] B. Goswami and A. Chatterjee, "Balancing a Stick With Eyes Shut: Inverted Pendulum on a Cart Without Angle Measurement," J. Dyn. Syst. Meas. Control, vol. 145, no. 4, Feb. 2023.
[21] S. Israilov et al., "Reinforcement learning approach to control an inverted pendulum: A general framework for educational purposes," PLoS One, vol. 18, no. 2, p. e0280071, Feb. 2023.
[22] S. Zeghlache, M. Z. Ghellab, A. Djerioui, B. Bouderah, and M. F. Benkhoris, "Adaptive fuzzy fast terminal sliding mode control for inverted pendulum-cart system with actuator faults," Math. Comput. Simul., vol. 210, pp. 207–234, 2023.
[23] G. M. Moatimid, A. T. El-Sayed, and H. F. Salman, "Dynamical analysis of an inverted pendulum with positive position feedback controller approximate uniform solution," Sci. Rep., vol. 13, no. 1, p. 8849, 2023.
[24] J.-J. E. Lopez, Brett T. and Slotine, "Contraction Metrics in Adaptive Nonlinear Control," *ArXiv*, 2020, doi: https://doi.org/10.48550/arxiv.1912.13138.
[25] B. T. Lopez and J.-J. E. Slotine, "Adaptive Nonlinear Control With Contraction Metrics," *IEEE Control Syst Lett*, vol. 5, no. 1, pp. 205–210, 2021, doi: 10.1109/LCSYS.2020.3000190.
[26] B. B. Sharma and I. N. Kar, "Contraction theory based adaptive synchronization of chaotic systems," *Chaos Solitons Fractals*, vol. 41, no. 5, pp. 2437–2447, 2009, doi: DOI:101016/jchaos200809031.
[27] W. LOHMILLER and J.-J. E. SLOTINE, "On Contraction Analysis for Non-linear Systems," *Automatica*, vol. 34, no. 6, pp. 683–696, 1998, doi: https://doi.org/10.1016/S0005-1098(98)00019-3.
[28] W. Lohmiller and J.-J. E. Slotine, "Control system design for mechanical systems using contraction theory," *IEEE Trans Automat Contr*, vol. 45, no. 5, pp. 984–989, 2000, doi: 10.1109/9.855568.
[29] I. R. Manchester and J.-J. E. Slotine, "Control Contraction Metrics: Convex and Intrinsic Criteria for Nonlinear Feedback Design," *IEEE Trans Automat Contr*, vol. 62, no. 6, pp. 3046–3053, 2017, doi: 10.1109/TAC.2017.2668380.
[30] X. Zhang and B. Cui, "Synchronization of Lurie system based on contraction analysis," *Appl Math Comput*, vol. 223, pp. 180–190, 2013, doi: https://doi.org/10.1016/j.amc.2013.07.080.
[31] A. Ouannas, I.M. Batiha, S. Bekiros, J. Liu, H. Jahanshahi, A.A. Aly, A.H. Alghtani, "Synchronization of the Glycolysis Reaction-Diffusion Model via Linear Control Law," Entropy, vol. 23, no. 11, p. 1516, Nov. 2021, doi: 10.3390/e23111516.
[32] A. Khooshehmehri, S. Nasrollahi, and M. Aliyari, "Chaos Synchronization in Josephson Junction Using a Nonlinear Model Predictive Controller Based on Particle Filter: Processor in the Loop Implementation," Int. J. Ind. Electron. Control Optim., vol. 4, no. 3, pp. 355–366, 2021.
[33] J. Y. Lau, W. Liang, and K. K. Tan, "Enhanced robust impedance control of a constrained piezoelectric actuator-based surgical device," Sensors Actuators A Phys., vol. 290, pp. 97–106, 2019.
[34] J. Y. Lau, W. Liang, and K. K. Tan, "Adaptive sliding mode enhanced disturbance observer-based control of surgical device," ISA Trans., vol. 90, pp. 178–188, 2019.
[35] M. Jalaeian-F, M. M. Fateh, M. Rahimiyan, M. Jalaeian-F., M. M. Fateh, and M. Rahimiyan, "Optimal Predictive Impedance Control in the Presence of Uncertainty for a Lower Limb Rehabilitation Robot," J. Syst. Sci. Complex., vol. 33, no. 3, pp. 1310–1329, May 2020.



Rogayeh Soltani is a Ph.D. candidate in Applied Mathematics at Payame Noor University (PNU). She is also with the Farhangian University of Tabriz as an instructor, since 2001. Her research interests include control, optimization, contraction theory, and control of chaotic systems.



Bashir Naderi received his Ph.D. in Applied Mathematics from Payame Noor University (PNU), Iran, in 2016. Now, he is an Assistant Professor of Mathematics at Payame Noor University (PNU), Iran. His main research interests include Dynamical systems, Optimal control, Chaotic systems, and Secure communications.



Saeed Nezhadhosein received his Ph.D. in Applied Mathematics from Pyame Noor University (PNU), Iran, in 2015. Now he is an Assistant Professor of Mathematics at Payame Noor University (PNU), Iran. His main research interests include Dynamical systems, Optimal control, and Nonlinear optimization.



Aghileh Heydari was born in 1972. She received her B.S. degree in Applied Mathematics in 1994 from Sharif University, Tehran, Iran, and her M.S. degree in Applied Mathematics (Optimal Control) in 1997 from Ferdowsi University of Mashhad (FUM), Iran. She wrote her dissertation under the supervision of Prof. Ali Vahidian Kamyad. She received her Ph.D. degree under the supervision of Prof. Ali Vahidian Kamyad at FUM in March 2002. She is currently a professor of Mathematics at Payame Noor University (PNU), Iran. PNU has numerous branches throughout Iran. Her research interests include Optimization, Optimal Control, Fuzzy Optimal Control Problems, Biomathematics, Modelling & Optimal Control of infectious diseases.